Towards a heterogeneous cable-connected team of UAVs for aerial manipulation

Vishal Abhishek, Vaibhav Srivastava, and Ranjan Mukherjee

***Abstract*— We study control of a heterogeneous team of two UAVs connected through a flexible cable such that the smaller UAV provides more accessibility in terms of reaching constrained locations, the larger UAV provides the base where heavier equipment can be installed, and the flexible cable acts as the conduit to carry electrical or communication cables, or for transporting fluids between the two UAVs. Our control design leverages the catenary model to compute the quasi-static cable tension and uses it to feedback linearize the system. An extended high-gain observer is used to estimate system states and to refine the estimate of cable tension. The estimates are used in the output feedback controller and the stability of the overall system is established. We illustrate the effectiveness of our methods using numerical simulations.**

I. INTRODUCTION

Unmanned Aerial Vehicles (UAVs) provide a very useful solution to perform tasks at remote locations such as inspection, surveillance, tool operation, or package delivery. With the advances in usage and technology, multiple UAVs are required to work cooperatively to perform a task.

In this paper, we consider a heterogeneous team of two UAVs connected together with a flexible cable such that the smaller (tool) UAV provides more accessibility in terms to reaching constrained locations, the larger (base) UAV provides the base where heavier equipment can be installed, and the flexible cable acts as the conduit to carry electrical or communication cables, or for transporting fluids between the two UAVs. Applications of such a system include high bandwidth sensing in which the smaller UAV carries sensors and tracks a trajectory to achieve desired spatio-temporal sensing footprint, and the collected high resolution data is sent to the data processing station on the larger UAV through the high bandwidth communication cable. Another example concerns cleaning windows of high-rise buildings or remotely located solar panels, wherein the larger UAV carries cleaning liquid reservoir, the cable transfers the liquid to the smaller UAV, which cleans the surface.

Several UAV-based manipulation systems have been designed, for example, for aerial pick and place [1], avian inspired grasping and perching [2, 3], mobile manipulation [4–6], assembly [7], valve turning [8]; see [9] for an extensive review. In [10], the authors consider a rigid rod-like object suspended at one end from a UAV through a spherical joint and study scenarios with both torque-actuated and actuation-free joint. In [11], the authors design a spherically connected multiquadrotor (SmQ) platform in which multiple quadrotors are used as rotating thrust generators for the platform. In [12], the authors design a dual arm connected at the tip of a flexible link attached to the UAV. In [13] and [14], a manipulator arm is connected at the end of a rod and a platform, respectively, which in turn are attached to the UAV through a passive spherical joint and act as a pendulum. In a companion paper [15], we design an extended high gain observer based output feedback control for multi-body multi-rotor based manipulation, where a birotor connected to a UAV through a rigid rod is considered.

Using cables to connect a load from a UAV has been considered extensively. Transporting a load using suspended cables has been considered both in single UAV [16–19] as well as multi-UAV scenarios [20–24]. Control of quadrotors with cable suspended payload using flexible cables has been studied and nonlinear geometric control has been designed in [25–27]. Differential flatness and geometric control of quadrotors with a payload suspended through flexible cables has been considered in [28]. Control of a UAV tethered to a taut cable fixed at one end is studied and an observer based control is discussed in [29, 30]. Here, the cable is assumed to be always taut and any flexibility is ignored. In [31] a geometric control of a tethered quadrotor is considered for tracking a desired trajectory while a linearization based controller stabilizes the flexible tether. In [32] multiple quadrotors carrying a flexible hose are considered. The cable is modeled as a series of lumped mass system and differential flatness of this system is studied. A linear time-varying LQR is designed to track desired trajectories assuming variation based linearized system. In contrast, our feedback linearizing control design relies on directly estimating cable tension using catenary model and subsequently refining it using the extended high gain observer to incorporate the influence of cable dynamics.

In this paper, we present the control of a cable connected dual-UAV system. The cable is assumed to be constant in length while flexible in its bending. We design an extended high gain observer (EHGO) based controller to track a desired trajectory of the tool and base UAVs. We use quasi-static tension in a cable under gravity obtained using catenary model as an estimate of cable tension. The estimate is refined using extended high gain observer to incorporate the influence of the cable dynamics. The state and cable tension estimates are used to design an output feedback controller, which is systematically analyzed. The proposed controller actively estimates and compensates cable tension leading to

This work was supported in part by ARO grant W911NF-18-1-0325.

V. Abhishek and R. Mukherjee are with the Department of Mechanical Engineering, Michigan State University, East Lansing, MI 48824-1226, USA {abhishe3,mukherji} at egr.msu.edu

V. Srivastava is with the Electrical and Computer Engineering, Michigan State University, East Lansing, MI 48824-1226, USA vaibhav at egr.msu.edu

decoupled dynamics for the base and the tool UAV . Thus, the controller can be independently applied to both UAVs. For simplicity of exposition, in the following we restrict the presentation to the case where the base UAV is hovering while the tool UAV tracks a desired trajectory.

The remainder of the paper is organized in the following way. Section II presents the design and modeling of the dual-UAV system. The EHGO-based control design and associated stability analysis are presented in Sections III and IV, respectively. Numerical simulations illustrating the effectiveness of the proposed controller are presented in Section V. Finally, Section VI concludes the paper.

II. System Modeling

We consider a team of two heterogeneous UAVs connected through a flexible cable such that one of the UAVs (referred as the tool UAV) tracks a desired trajectory while the other UAV (referred as the base UAV) provides the required thrust. The resulting system referred as cable connected dual-UAV system is shown in Fig. 1. We focus on the case where the base UAV is hovering. Our controller design decouples the two UAVs by canceling the estimated tension due to the cable at both UAVs. Therefore, we focus on control of the tool UAV only. A similar controller can be designed for the base UAV as well. For further analysis, we restrict to the case of planar motion in a vertical plane. We use catenary equations which yield the tension in the cable assuming static equilibrium under gravity.

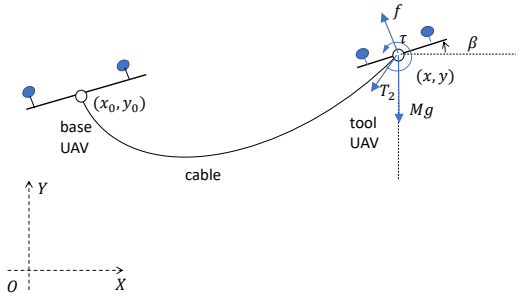

Fig. 1. Cable connected dual-UAV system

A. Catenary Model

To compute the tension in the cable we use the catenary model [33, chapter 10] which provides the shape as well as the tension in the cable fixed at the two ends assuming static equilibrium under gravity. Let λ be the mass per unit length of the cable, g acceleration due to gravity, s be the distance along the length of the cable, varying from $s = 0$ at one end point $P_0 = (x_0, y_0)$ and $s = L$ at the other end point $P = (x, y)$. The tension in the cable at any point is given in terms of three parameters of the curve: a, x_c and y_c. These parameters can be determined by using the coordinates of the two end points. Below we give the expressions for these parameters. The parameter a is obtained by solving the following transcendental equation

$$\sqrt{L^2 - (y - y_0)^2} = 2a \sinh \frac{|x - x_0|}{2a}.$$

The expressions for x_c and y_c are given by

$$x_c = x_0 + \text{sign}(x - x_0)\ a \log\Big(\frac{D \mp \sqrt{D^2 - 4E}}{2}\Big),$$
$$y_c = y_0 - a \cosh \frac{x - x_c}{a},$$

where, in the above expression for x_c, the sign in the argument of $\log(\cdot)$ is selected negative if $y - y_0 \geq 0$ and positive if $y - y_0 < 0$. The expressions for D and E used above are given by

$$D = 2L \frac{\exp(|x - x_0|/a)}{a(\exp(|x - x_0|/a) - 1)}; \quad E = \exp(|x - x_0|/a).$$

The tension at the end P for the case when $x - x_0 \neq 0$ is given by

$$T_x^c = \text{sign}(x - x_0)\ \lambda g a, \qquad T_y^c = \lambda g \sqrt{(y - y_c)^2 - a^2},$$

while for the case when $x - x_0 = 0$, we have

$$T_x^c = 0, \qquad T_y^c = \lambda g \frac{L + (y - y_0)}{2}.$$

B. Dynamic Model of the tool UAV

We assume that the cable is connected to the two UAVs at their respective centers of mass. The system alongwith the forces at the tool UAV can be seen in Fig. 1. We adopt the following notation

M	mass of the tool UAV
I	moment of inertia of the tool UAV about Z axis passing through its center of mass
m	mass of the cable
L	length of the cable
(x, y)	position coordinates of the tool UAV in the inertial frame
β	angular position of the tool UAV
f	rotor thrust on the tool UAV
T_2	cable tension at the tool UAV with components T_x and T_y in x and y direction, respectively
τ	rotor moment on the tool UAV about its center
g	acceleration due to gravity

The equations of motion of the tool UAV are

$$\begin{aligned} M\ddot{x} &= -f \sin\beta - T_x, \\ M\ddot{y} &= f \cos\beta - T_y - Mg, \\ I\ddot{\beta} &= \tau. \end{aligned} \tag{2}$$

Let $\sigma_x := \frac{1}{M}(T_x - T_x^c)$, $\sigma_y := \frac{1}{M}(T_y - T_y^c)$ be the difference between the tension computed using quasi-static catenary equations and the actual cable tension. Define $\boldsymbol{q}_1 = [x, y]^\top$, $\boldsymbol{q}_2 = \dot{\boldsymbol{q}}_1$, $\boldsymbol{\sigma}_q := [\sigma_x, \sigma_y]^\top$ and $\boldsymbol{q} = [\boldsymbol{q}_1^\top, \boldsymbol{q}_2^\top]^\top$. Let $\dot{\boldsymbol{\sigma}}_q := \boldsymbol{\varphi}_{\boldsymbol{q}}(t, \boldsymbol{q})$, where $\boldsymbol{\varphi}_{\boldsymbol{q}}(t, \boldsymbol{q})$ is an unknown function which is continuous and bounded on any compact subset of $\mathbb{R}_{\geq 0} \times \mathbb{R}^4$.

III. Control Design

We design an EHGO based output feedback control to track a desired trajectory for the tool UAV position coordinates. Let the desired trajectory be $\boldsymbol{q}_1^d(t) = [x^d(t), y^d(t)]^\top$ and define tracking error $\boldsymbol{e}_1 := \boldsymbol{q}_1^d - \boldsymbol{q}_1 = [e_x, e_y]^\top$, $\boldsymbol{e}_2 := \dot{\boldsymbol{e}}_1$ and $\boldsymbol{e} := [(\boldsymbol{e}_1)^\top, (\boldsymbol{e}_2)^\top]^\top$. We assume feedback available in position and orientation of the tool UAV, namely, outputs $\boldsymbol{q}_1$ and β. We begin with state feedback control design.

A. State Feedback Control

The position error dynamics can be written using (2) as

$$\ddot{\boldsymbol{e}}_1 = \ddot{\boldsymbol{q}}_1^d - \begin{bmatrix} -\frac{f}{M}\sin\beta - \frac{T_x^c}{M} - \sigma_x \\ \frac{f}{M}\cos\beta - \frac{T_y^c}{M} - g - \sigma_y \end{bmatrix}.$$

Here we have written T_x as $T_x^c + M\sigma_x$ and T_y as $T_y^c + M\sigma_y$. Now, assuming the state as well as disturbance signals σ_x and σ_y are known, it can be seen that designing a control law such that

$$\begin{bmatrix} -f\sin\beta \\ f\cos\beta \end{bmatrix} = M(\ddot{\boldsymbol{q}}_1^d + K_1\boldsymbol{e}_1 + K_2\dot{\boldsymbol{e}}_1) + \begin{bmatrix} T_x^c + M\sigma_x \\ T_y^c + Mg + M\sigma_y \end{bmatrix},$$

linearizes the position tracking error dynamics. Thus,

$$f = \left\| M(\ddot{\boldsymbol{q}}_1^d + K_1\boldsymbol{e}_1 + K_2\dot{\boldsymbol{e}}_1) + \begin{bmatrix} T_x^c + M\sigma_x \\ T_y^c + Mg + M\sigma_y \end{bmatrix} \right\|, \tag{3a}$$

$$\beta^c = \operatorname{atan}_2\Big(-M(\ddot{x}^d + K_1 e_x + K_2\dot{e}_x) - T_x^c - M\sigma_x, \\ M(\ddot{y}^d + K_1 e_y + K_2\dot{e}_y) + T_y^c + Mg + M\sigma_y \Big), \tag{3b}$$

where $\operatorname{atan}_2(\cdot)$ is the 2-argument arc tangent function. The commanded value β^c will be used as the desired trajectory for the orientation dynamics. The orientation dynamics of the UAV are written through the following change of variables

$$\tilde{\beta}_1 = \beta^c - \beta, \quad \tilde{\beta}_2 = \dot{\tilde{\beta}}_1 = \dot{\beta}^c - \dot{\beta}, \quad \tilde{\boldsymbol{\beta}} = [\tilde{\beta}_1, \tilde{\beta}_2]^\top,$$

leading to

$$\dot{\tilde{\beta}}_1 = \tilde{\beta}_2, \tag{4a}$$

$$\dot{\tilde{\beta}}_2 = \frac{-\tau}{I} + \ddot{\beta}^c. \tag{4b}$$

We set the control input f as given by (3a) and τ as

$$\tau = I(K_3\tilde{\beta}_1 + K_4\tilde{\beta}_2 + \ddot{\beta}^c). \tag{5}$$

The closed-loop system dynamics then becomes

$$\dot{\boldsymbol{e}} = A_{\boldsymbol{e}}\boldsymbol{e} + \begin{bmatrix} 0_2 \\ \boldsymbol{e}_\beta(t, \boldsymbol{e}, \tilde{\beta}_1) \end{bmatrix}, \tag{6a}$$

$$\dot{\tilde{\boldsymbol{\beta}}} = A_{\tilde{\boldsymbol{\beta}}}\tilde{\boldsymbol{\beta}}, \tag{6b}$$

where

$$A_{\boldsymbol{e}} = \begin{bmatrix} 0_{2\times2} & I_{2\times2} \\ -K_1 I_{2\times2} & -K_2 I_{2\times2} \end{bmatrix}, \quad A_{\tilde{\boldsymbol{\beta}}} = \begin{bmatrix} 0 & 1 \\ -K_3 & -K_4 \end{bmatrix},$$

$$\boldsymbol{e}_\beta(t, \boldsymbol{e}, \tilde{\beta}_1) = \frac{f}{M}\begin{bmatrix} \sin(\beta^c - \tilde{\beta}_1) - \sin\beta^c \\ \cos\beta^c - \cos(\beta^c - \tilde{\beta}_1) \end{bmatrix}.$$

Note that $\boldsymbol{e}_\beta(t, \boldsymbol{e}, 0) = 0$ for all $t > 0$. In the state feedback control law as designed above we need states $\boldsymbol{e}_1$, $\tilde{\boldsymbol{\beta}}$ and feedforward term $\ddot{\boldsymbol{q}}_1^d$ which are known through measurement or by design along with states $\boldsymbol{e}_2$ and $\tilde{\boldsymbol{\beta}}_2$, disturbance signals σ_x and σ_y, and feedforward term $\ddot{\beta}^c$ which we assume unknown and estimate using extended high gain observer in the next section.

B. Extended High-Gain Observer Design

We design an extended high-gain observer (EHGO) to estimate unmeasured states as well as uncertainties in the form of modeling error and external disturbances. These estimates will be used to cancel out the uncertainties in the control design, resulting in improved performance of the feedback linearizing controllers. We begin by noting from the previous subsection that the control input τ for a state feedback based linearizing controller requires the computation of $\ddot{\beta}^c$. In order to avoid this, we lump this quantity with any disturbance in the right hand side of (4b) to arrive at

$$\dot{\tilde{\beta}}_1 = \tilde{\beta}_2, \tag{7a}$$

$$\dot{\tilde{\beta}}_2 = \frac{-\tau}{I} + \sigma_\beta. \tag{7b}$$

The new state feedback linearizing control law for rotational dynamics will be $\tau = I(K_3\tilde{\beta}_1 + K_4\tilde{\beta}_2 + \sigma_\beta)$. We treat σ_β as a state and assume $\dot{\sigma}_\beta = \varphi_\beta(t, \tilde{\boldsymbol{\beta}})$, where $\varphi_\beta(t, \tilde{\boldsymbol{\beta}})$ is an unknown function that is continuous and bounded on any compact subset of $\mathbb{R}_{\geq 0} \times (-\frac{\pi}{2}, \frac{\pi}{2})$.

Define $\boldsymbol{\chi} = [(\boldsymbol{e}_1)^\top, (\boldsymbol{e}_2)^\top, (\boldsymbol{\sigma_q})^\top, \tilde{\beta}_1, \tilde{\beta}_2, \sigma_\beta]^\top \in \mathbb{R}^9$,

$$A = \begin{bmatrix} 0_{2\times2} & I_{2\times2} & 0_{2\times2} \\ 0_{2\times2} & 0_{2\times2} & I_{2\times2} \\ 0_{2\times2} & 0_{2\times2} & 0_{2\times2} \end{bmatrix} \oplus \begin{bmatrix} 0 & 1 & 0 \\ 0 & 0 & 1 \\ 0 & 0 & 0 \end{bmatrix}, H = \begin{bmatrix} \rho_1/\epsilon I_2 \\ \rho_2/\epsilon^2 I_2 \\ \rho_3/\epsilon^3 I_2 \end{bmatrix} \oplus \begin{bmatrix} \rho_1/\epsilon \\ \rho_2/\epsilon^2 \\ \rho_3/\epsilon^3 \end{bmatrix},$$

and $C = \begin{bmatrix} I_{2\times2} & 0_{2\times2} & 0_{2\times2} \end{bmatrix} \oplus \begin{bmatrix} 1 & 0 & 0 \end{bmatrix}$,

where $\oplus$ denotes matrix direct sum, $\epsilon > 0$ is some sufficiently small constant and ρ_i's are selected such that

$$s^3 + \rho_1 s^2 + \rho_2 s + \rho_3 = 0,$$

is Hurwitz. Then, the combined system dynamics can be written with states $\boldsymbol{\chi}$ as

$$\dot{\boldsymbol{\chi}} = A\boldsymbol{\chi} + g(t, \beta, f, \tau, T_x^c, T_y^c) + \begin{bmatrix} 0_{4\times1} \\ \boldsymbol{\varphi_q} \\ 0_{2\times1} \\ \varphi_\beta \end{bmatrix}, \tag{8a}$$

$$\boldsymbol{y} = C\boldsymbol{\chi}, \tag{8b}$$

where

$$g(t, \beta, f, \tau, T_x^c, T_y^c) = \begin{bmatrix} 0_2 \\ \ddot{x}^d(t) - \frac{1}{M}(-f\sin\beta - T_x^c) \\ \ddot{y}^d(t) - \frac{1}{M}(f\cos\beta - T_y^c - Mg) \\ 0_2 \\ 0 \\ -\frac{\tau}{I} \\ 0 \end{bmatrix}.$$

The EHGO for the above combined system dynamics can now be written as

$$\dot{\hat{\boldsymbol{\chi}}} = A\hat{\boldsymbol{\chi}} + g(t,\beta,f,\tau,T_x^c,T_y^c) + H\hat{\boldsymbol{y}}_e, \tag{9a}$$

$$\hat{\boldsymbol{y}}_e = C(\boldsymbol{\chi} - \hat{\boldsymbol{\chi}}). \tag{9b}$$

where $\hat{\boldsymbol{\chi}} = [(\hat{\boldsymbol{e}}_1)^\top, (\hat{\boldsymbol{e}}_2)^\top, \hat{\boldsymbol{\sigma}}_q, \hat{\tilde{\beta}}_1, \hat{\tilde{\beta}}_2, \hat{\sigma}_\beta]^T \in \mathbb{R}^9$ is the estimate of $\boldsymbol{\chi}$. We can now define an output-feedback controller to ensure tracking of the trajectory $\boldsymbol{q}^d(t)$. The output-feedback controller is designed using the estimates from the EHGO as

$$f = \left\| M(\ddot{\boldsymbol{q}}_1^d + K_1\boldsymbol{e} + K_2\hat{\boldsymbol{e}}_2) + \begin{bmatrix} T_x^c + M\hat{\sigma}_x \\ T_y^c + Mg + M\hat{\sigma}_y \end{bmatrix} \right\|, \tag{10a}$$

$$\tau = I(K_3\tilde{\beta}_1 + K_4\hat{\tilde{\beta}}_2 + \hat{\sigma}_\beta), \tag{10b}$$

with commanded angle β^c now given by

$$\beta^c = \operatorname{atan}_2\Big(-M(\ddot{x}^d + K_1 e_x + K_2\hat{\dot{e}}_x) - T_x^c - M\hat{\sigma}_x, \\ M(\ddot{y}^d + K_1 e_y + K_2\hat{\dot{e}}_y) + T_y^c + Mg + M\hat{\sigma}_y\Big),$$

where $[\hat{\dot{e}}_x, \hat{\dot{e}}_y]^\top = \hat{\boldsymbol{e}}_2$ and $[\hat{\sigma}_x, \hat{\sigma}_y]^\top = \hat{\boldsymbol{\sigma}}_q$.

IV. Stability Analysis

The stability of the state feedback control, observer estimates, and output feedback controller will now be proven. We begin by restricting the domain of operation by establishing a compact positively invariant set. We then prove stability of the closed-loop system under state feedback, convergence of the observer estimates, and finally prove stability of the closed-loop system under output feedback.

A. Restricting Domain of Operation

Note that when the cable is taut and not in a vertical alignment, i.e. $x \neq x_0$, the catenary model no longer holds and there is a singularity in the motion of the UAVs. Also, at such configurations the cable tension as per the catenary model becomes unbounded. In order to prevent the cable from being taut, the distance between the two UAVs must remain stricly smaller than the cable length L. To restrict the domain of operation such that $(x-x_0)^2 + (y-y_0)^2 \leq L^*$, where $L^* < L$, we make the following assumption about the desired trajectory of the tool UAV

$$(x^d - x_0)^2 + (y^d - y_0)^2 < L^* - \delta_e. \tag{11}$$

If the position tracking error $\|\boldsymbol{e}_1\| \leq \delta_e$, then the above assumption ensures that the tool UAV remains in the desired domain of operation. Further to restrict the rotational angle β such that $-\pi/2 < \beta < \pi/2$, we assume the following restriction on the commanded angle $|\beta^c| \leq \pi/2 - \delta$, which means if the rotational tracking error $\|\tilde{\beta}\| \leq \delta$, then the requirement on β is satisfied. For the state feedback controlled system (6), we show below that there exist a consistent choice of δ_e and δ, and a positively invariant compact set $\Omega = \Omega_e \times \Omega_{\tilde{\beta}}$, such that if the initial tracking error lie in Ω, then $\|\boldsymbol{e}_1(t)\| \leq \delta_e$ and $\|\tilde{\beta}(t)\| \leq \delta$.

Consider the following Lyapunov function for the rotational error dynamics

$$V_{\tilde{\boldsymbol{\beta}}} = \tilde{\boldsymbol{\beta}}^\top P_{\tilde{\boldsymbol{\beta}}}\tilde{\boldsymbol{\beta}}, \quad \text{where} \quad P_{\tilde{\boldsymbol{\beta}}}A_{\tilde{\boldsymbol{\beta}}} + A_{\tilde{\boldsymbol{\beta}}}^\top P_{\tilde{\boldsymbol{\beta}}} = -I_2. \tag{12}$$

Since $A_{\tilde{\boldsymbol{\beta}}}$ is Hurwitz, a symmetric positive definite $P_{\tilde{\boldsymbol{\beta}}}$ as defined above exists. Further,

$$\lambda_{\min}(P_{\tilde{\boldsymbol{\beta}}})\|\tilde{\boldsymbol{\beta}}\|^2 \leq V_{\tilde{\boldsymbol{\beta}}} \leq \lambda_{\max}(P_{\tilde{\boldsymbol{\beta}}})\|\tilde{\boldsymbol{\beta}}\|^2, \quad \dot{V}_{\tilde{\boldsymbol{\beta}}} = -\|\tilde{\boldsymbol{\beta}}\|^2.$$

Define $\Omega_{\tilde{\boldsymbol{\beta}}} = \{V_{\tilde{\boldsymbol{\beta}}} \leq c_{\tilde{\boldsymbol{\beta}}}\}$. It can be seen from above that $\Omega_{\tilde{\boldsymbol{\beta}}}$ is a positively invariant set. Now, taking $c_{\tilde{\boldsymbol{\beta}}} = \lambda_{\min}(P_{\tilde{\boldsymbol{\beta}}})\delta^2$, implies $\|\tilde{\boldsymbol{\beta}}\| \leq \delta$ and hence $\|\tilde{\beta}\| \leq \delta$ as required.

Similar to the rotational dynamics, consider the following Lyapunov function for the position dynamics

$$V_{\boldsymbol{e}} = \boldsymbol{e}^\top P_{\boldsymbol{e}}\boldsymbol{e}, \quad \text{where} \quad P_{\boldsymbol{e}}A_{\boldsymbol{e}} + A_{\boldsymbol{e}}^\top P_{\boldsymbol{e}} = -I_4. \tag{13}$$

Taking derivative,

$$\begin{aligned} \dot{V}_{\boldsymbol{e}} &= -\|\boldsymbol{e}\|^2 + 2[\boldsymbol{0}_2^\top, \boldsymbol{e}_\beta^\top]P_{\boldsymbol{e}}\boldsymbol{e} \\ &\leq -\|\boldsymbol{e}\|^2 + 2\lambda_{\max}(P_{\boldsymbol{e}})\|\boldsymbol{e}_\beta\|\|\boldsymbol{e}\|. \end{aligned} \tag{14}$$

Since $\boldsymbol{e}_\beta(t,\tilde{\beta})$, written as function of time t and $\tilde{\beta}$, is continous and uniformly bounded in t (as all signals remain bounded under bounded desired trajectory assumption) and its partial derivative with respect to $\tilde{\beta}$ is continous, $\boldsymbol{e}_\beta(t,\tilde{\beta})$ is Lipschitz in $\tilde{\beta}$ on $\Omega_{\tilde{\beta}}$. Hence, in $\Omega_{\tilde{\beta}}$

$$\|\boldsymbol{e}_\beta(\tilde{\beta}) - \boldsymbol{e}_\beta(0)\| \leq L\|\tilde{\beta}\| \leq L\delta, \tag{15}$$

which yields

$$\dot{V}_{\boldsymbol{e}} \leq -\|\boldsymbol{e}\|^2 + 2\lambda_{\max}(P_{\boldsymbol{e}})L\delta\|\boldsymbol{e}\|. \tag{16}$$

Therefore, for $\|\boldsymbol{e}\| > 2\lambda_{\max}(P_{\boldsymbol{e}})L\delta$, $\dot{V}_{\boldsymbol{e}} < 0$. Using this with the fact that $\lambda_{\min}(P_{\boldsymbol{e}})\|\boldsymbol{e}\|^2 \leq V_{\boldsymbol{e}} \leq \lambda_{\max}(P_{\boldsymbol{e}})\|\boldsymbol{e}\|^2$ makes $\Omega_{\boldsymbol{e}} = \{V_{\boldsymbol{e}} \leq c_{\boldsymbol{e}}\}$ positively invariant with a choice of $c_{\boldsymbol{e}}$ satisfying

$$c_{\boldsymbol{e}} \geq \lambda_{\max}(P_{\boldsymbol{e}})(2\lambda_{\max}(P_{\boldsymbol{e}})L\delta)^2. \tag{17}$$

Therefore, the domain of operation defined as $\Omega = \Omega_{\boldsymbol{e}} \times \Omega_{\tilde{\boldsymbol{\beta}}}$, is compact and positively invariant under state feedback.

Note that choosing $c_{\boldsymbol{e}} = \lambda_{\min}(P_{\boldsymbol{e}})\delta_e^2$ implies $\|\boldsymbol{e}_1\| \leq \delta_e$. Therefore, the choice of two error tolerances δ_e and δ must satisfy

$$\lambda_{\min}(P_{\boldsymbol{e}})\delta_e^2 \geq \lambda_{\max}(P_{\boldsymbol{e}})(2\lambda_{\max}(P_{\boldsymbol{e}})L\delta)^2.$$

Hence, for a given choice of error tolerances satisfying the above, if the initial tracking errors satisfy $\|\boldsymbol{e}(0)\| \leq \sqrt{\lambda_{\min}(P_{\boldsymbol{e}})/\lambda_{\max}(P_{\boldsymbol{e}})}\delta_e$ and $\|\tilde{\boldsymbol{\beta}}(0)\| \leq \sqrt{\lambda_{\min}(P_{\tilde{\boldsymbol{\beta}}})/\lambda_{\max}(P_{\tilde{\boldsymbol{\beta}}})}\delta$, then $(\boldsymbol{e}(0), \tilde{\boldsymbol{\beta}}(0)) \in \Omega$, and hence $\|\boldsymbol{e}_1(t)\| \leq \delta_e$ and $\|\tilde{\beta}(t)\| \leq \delta$.

B. Stability under State Feedback

Lemma 1 (Stability under State Feedback): For the closed-loop system under state feedback (6), with initial tracking error $(\boldsymbol{e}(0), \tilde{\boldsymbol{\beta}}(0))$ in Ω, the system states $(\boldsymbol{e}(t), \tilde{\boldsymbol{\beta}}(t))$ remain in Ω for all $t > 0$ and exponentially converge to the origin.

Proof: Taking a composite Lyapunov function

$$V = dV_e + V_{\tilde{\beta}}, \quad d > 0 \tag{18}$$

and following the generalized proof for cascaded system stability in the Appendix of [34], it can be shown that the closed-loop state feedback system given by (6) converges exponentially to the origin for d chosen small enough. ■

C. Stability of Output Feedback

The system under output feedback is a singularly perturbed system which can be split into two time-scales. The system dynamics and control reside in the slow time-scale while the observer resides in the fast time-scale. The observer estimates can be shown to converge to an $O(\epsilon)$ neighborhood of the true estimates.

Lemma 2 (Convergence of EHGO Estimates): The observer estimates $\hat{\boldsymbol{\chi}}$ converge exponentially to an $O(\epsilon)$ neighborhood of the true states $\boldsymbol{\chi}$, for any $\epsilon \in (0, \epsilon^*)$ for sufficiently small $\epsilon^* > 0$.

The lemma can be proved following the standard high gain observer proof given in [35].

Theorem 1 (Stability under Output Feedback): The closed-loop system under output feedback, with initial conditions in the interior of Ω, exponentially converges to an $O(\epsilon)$ neighborhood of the origin when ϵ is chosen small enough.

Proof: The proof follows the standard arguments used in the stability analysis of extended high gain observer based output feedback control [35] and utilises the facts that state-feedback controlled error system is exponentially stable over a compact invariant domain of operation (Lemma 1), the observer dynamics reside in a faster timescale, and the observer estimates exponentially converge to an $O(\epsilon)$ neighborhood of the true states (Lemma 2). ■

V. Simulations

We perform simulations where we track a desired trajectory for the tool UAV position coordinates x, y. To compute the tension which is canceled in the control laws, we use the quasi-static catenary equations presented in II-A. These equations estimate the tension at both the ends of the cable assuming these ends to be fixed and use the position coordinates of the two ends. In these simulations, we keep the base UAV end fixed and treat it as the origin, however, a disturbance on the base UAV position is added to account for more realistic conditions in which oscillations around the hovering position occur. The position of the base UAV is known to the tool UAV either through a central unit or through a sensor. Note that in the quasi-static calculations of cable tension, only the relative position of the two ends of the cable matters. In order to simulate the dynamics of the flexible cable, we use the discretized lumped mass model of [32] with one end of the cable attached to the base UAV and the other attached to the tool UAV. The cable length is taken as $10\ m$ with mass per unit length $\lambda = 0.5\ kg/m$. We have considered equidistant discretization into 10 segments where the mass of the segment is considered lumped at the discretization points. We select a desired trajectory in position coordinates from time $t = 0$ to $10\ s$, with $0 - 5\ s$ as 9th order polynomial in time such that the tool end covers a displacement of $2\ m$ in each of the coordinates and have derivatives upto 5th order as 0 at initial time $t = 0\ s$ and time $t = 5\ s$. We keep the desired coordinates fixed at $2\ m$ from the start position for time $5 - 10\ s$. The trajectory is chosen so as to have the smoothness requirement of upto fifth order derivatives since the control law involves second order derivatives of β^c which further involves fourth order derivatives of the desired trajectory. The initial coordinates of the tool UAV is set as $x = 5\ m$, $y = 0\ m$ relative to the base UAV. We also add a disturbance in the position of the base UAV as a sinusoidal signal: $0.1 \sin t$ in both x and y coordinates. We begin with simulations of full state feedback control using control law as per (3a), (3b) and (5). Here, we have assumed the difference in cable tension due to cable dynamics, i.e., σ_x and σ_y as zero, while for computation of $\ddot{\beta}^c$ we have used numerical differentiation using backward difference algorithm. The plots for trajectory tracking for the case of state feedback (SF) as well as EHGO based control are shown in Fig. 2. As can be seen from the plots, the system is able to closely track the desired trajectory and the tracking error goes to zero. Figure 2(b) and Fig. 2(c) show the plots of tracking error for SF based control as well as EHGO based control. The tracking in EHGO case can be seen to be better than the state feedback control.

VI. Conclusions

We consider control of a team of two UAVs connected through a flexible cable. We design an extended high gain observer based output feedback control where the output available through sensing are the UAV position and angular coordinates. We use the catenary model to compute the quasi-static cable tension and cancel it in our control law. The difference between the quasi-static cable tension and the actual tension is assumed to be a disturbance and is estimated by the extended high gain observer. We numerically illustrate the effectiveness of the proposed approach in the presence of external disturbances. In this work, we have considered the case where the system is restricted to move in a plane. The future work includes extension of these results to three-dimensional environments.

References

[1] G. Garimella and M. Kobilarov, "Towards model-predictive control for aerial pick-and-place," in *2015 IEEE International Conference on Robotics and Automation (ICRA)*, pp. 4692–4697, IEEE, 2015.

[2] J. Thomas, J. Polin, K. Sreenath, and V. Kumar, "Avian-inspired grasping for quadrotor micro UAVs," in *ASME 2013 International Design Engineering Technical Conferences and Computers and Information in Engineering Conference*, American Society of Mechanical Engineers Digital Collection, 2013.

[3] J. Thomas, G. Loianno, K. Sreenath, and V. Kumar, "Toward image based visual servoing for aerial grasping and perching," in *2014*

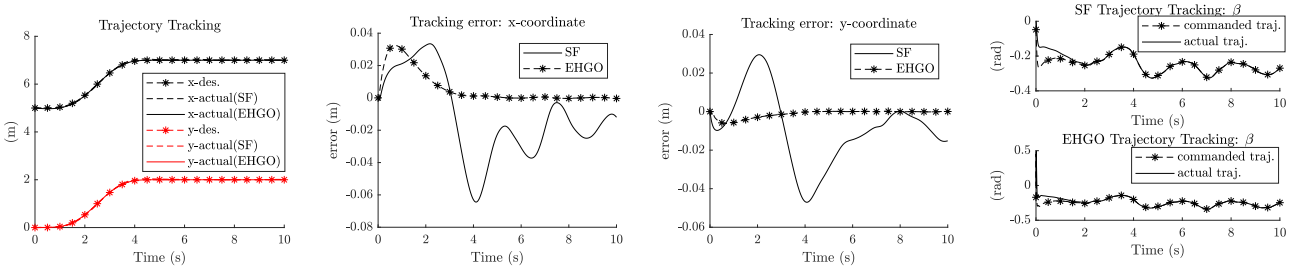

(a) Desired and actual trajectories (b) Tracking error: x (c) Tracking error: y (d) Commanded and actual values: β

Fig. 2. Trajectory tracking for position: x and y.

IEEE International Conference on Robotics and Automation (ICRA), pp. 2113–2118, IEEE, 2014.

[4] M. Orsag, C. Korpela, and P. Oh, "Modeling and control of MM-UAV: Mobile manipulating unmanned aerial vehicle," *Journal of Intelligent & Robotic Systems*, vol. 69, no. 1-4, pp. 227–240, 2013.

[5] S. Kim, S. Choi, and H. J. Kim, "Aerial manipulation using a quadrotor with a two dof robotic arm," in *2013 IEEE/RSJ International Conference on Intelligent Robots and Systems*, pp. 4990–4995, IEEE, 2013.

[6] G. Heredia, A. Jimenez-Cano, I. Sanchez, D. Llorente, V. Vega, J. Braga, J. Acosta, and A. Ollero, "Control of a multirotor outdoor aerial manipulator," in *2014 IEEE/RSJ International Conference on Intelligent Robots and Systems*, pp. 3417–3422, IEEE, 2014.

[7] A. Jimenez-Cano, J. Martin, G. Heredia, A. Ollero, and R. Cano, "Control of an aerial robot with multi-link arm for assembly tasks," in *2013 IEEE International Conference on Robotics and Automation*, pp. 4916–4921, IEEE, 2013.

[8] C. Korpela, M. Orsag, and P. Oh, "Towards valve turning using a dual-arm aerial manipulator," in *2014 IEEE/RSJ International Conference on Intelligent Robots and Systems*, pp. 3411–3416, IEEE, 2014.

[9] F. Ruggiero, V. Lippiello, and A. Ollero, "Aerial manipulation: A literature review," *IEEE Robotics and Automation Letters*, vol. 3, no. 3, pp. 1957–1964, 2018.

[10] P. O. Pereira and D. V. Dimarogonas, "Pose and position trajectory tracking for aerial transportation of a rod-like object," *Automatica*, vol. 109, p. 108547, 2019.

[11] H.-N. Nguyen, S. Park, J. Park, and D. Lee, "A novel robotic platform for aerial manipulation using quadrotors as rotating thrust generators," *IEEE Transactions on Robotics*, vol. 34, no. 2, pp. 353–369, 2018.

[12] A. Suarez, A. Giordano, K. Kondak, G. Heredia, and A. Ollero, "Flexible link long reach manipulator with lightweight dual arm: Soft-collision detection, reaction, and obstacle localization," in *2018 IEEE International Conference on Soft Robotics (RoboSoft)*, pp. 406–411, IEEE, 2018.

[13] A. Suárez, P. Sanchez-Cuevas, M. Fernandez, M. Perez, G. Heredia, and A. Ollero, "Lightweight and compliant long reach aerial manipulator for inspection operations," in *2018 IEEE/RSJ International Conference on Intelligent Robots and Systems (IROS)*, pp. 6746–6752, IEEE, 2018.

[14] M. J. Kim, J. Lin, K. Kondak, D. Lee, and C. Ott, "Oscillation damping control of pendulum-like manipulation platform using moving masses," *IFAC-PapersOnLine*, vol. 51, no. 22, pp. 465–470, 2018.

[15] C. J. Boss*, V. Abhishek*, and V. Srivastava, "Towards multi-body multi-rotors for long reach manipulation," in *American Control Conference (ACC)*, 2021. to appear.

[16] K. Sreenath, T. Lee, and V. Kumar, "Geometric control and differential flatness of a quadrotor UAV with a cable-suspended load," in *52nd IEEE Conference on Decision and Control*, pp. 2269–2274, IEEE, 2013.

[17] P. J. Cruz and R. Fierro, "Cable-suspended load lifting by a quadrotor UAV: hybrid model, trajectory generation, and control," *Autonomous Robots*, vol. 41, no. 8, pp. 1629–1643, 2017.

[18] P. O. Pereira, M. Herzog, and D. V. Dimarogonas, "Slung load transportation with a single aerial vehicle and disturbance removal," in *2016 24th Mediterranean Conference on Control and Automation (MED)*, pp. 671–676, IEEE, 2016.

[19] S. Dai, T. Lee, and D. S. Bernstein, "Adaptive control of a quadrotor uav transporting a cable-suspended load with unknown mass," in *53rd IEEE Conference on Decision and Control*, pp. 6149–6154, IEEE, 2014.

[20] N. Michael, J. Fink, and V. Kumar, "Cooperative manipulation and transportation with aerial robots," *Autonomous Robots*, vol. 30, no. 1, pp. 73–86, 2011.

[21] T. Lee, "Geometric control of quadrotor UAVs transporting a cable-suspended rigid body," *IEEE Transactions on Control Systems Technology*, vol. 26, no. 1, pp. 255–264, 2017.

[22] P. O. Pereira and D. V. Dimarogonas, "Nonlinear pose tracking controller for bar tethered to two aerial vehicles with bounded linear and angular accelerations," in *2017 IEEE 56th Annual Conference on Decision and Control (CDC)*, pp. 4260–4265, IEEE, 2017.

[23] D. Sanalitro, H. J. Savino, M. Tognon, J. Cortés, and A. Franchi, "Full-pose manipulation control of a cable-suspended load with multiple UAVs under uncertainties," *IEEE Robotics and Automation Letters*, 2020.

[24] M. Tognon, C. Gabellieri, L. Pallottino, and A. Franchi, "Aerial co-manipulation with cables: The role of internal force for equilibria, stability, and passivity," *IEEE Robotics and Automation Letters*, vol. 3, no. 3, pp. 2577–2583, 2018.

[25] F. A. Goodarzi and T. Lee, "Dynamics and control of quadrotor UAVs transporting a rigid body connected via flexible cables," in *2015 American Control Conference (ACC)*, pp. 4677–4682, IEEE, 2015.

[26] F. A. Goodarzi, D. Lee, and T. Lee, "Geometric control of a quadrotor UAV transporting a payload connected via flexible cable," *International Journal of Control, Automation and Systems*, vol. 13, no. 6, pp. 1486–1498, 2015.

[27] F. A. Goodarzi and T. Lee, "Stabilization of a rigid body payload with multiple cooperative quadrotors," *Journal of Dynamic Systems, Measurement, and Control*, vol. 138, no. 12, 2016.

[28] P. Kotaru, G. Wu, and K. Sreenath, "Differential-flatness and control of quadrotor(s) with a payload suspended through flexible cable(s)," in *2018 Indian Control Conference (ICC)*, pp. 352–357, IEEE, 2018.

[29] S. Lupashin and R. D'Andrea, "Stabilization of a flying vehicle on a taut tether using inertial sensing," in *2013 IEEE/RSJ International Conference on Intelligent Robots and Systems*, pp. 2432–2438, IEEE, 2013.

[30] M. Tognon and A. Franchi, "Nonlinear observer-based tracking control of link stress and elevation for a tethered aerial robot using inertial-only measurements," in *2015 IEEE International Conference on Robotics and Automation (ICRA)*, pp. 3994–3999, IEEE, 2015.

[31] T. Lee, "Geometric controls for a tethered quadrotor UAV," in *2015 54th IEEE Conference on Decision and Control (CDC)*, pp. 2749–2754, IEEE, 2015.

[32] P. Kotaru and K. Sreenath, "Multiple quadrotors carrying a flexible hose: dynamics, differential flatness and control," *arXiv preprint arXiv:1911.12650*, 2019.

[33] E. J. Routh, *A Treatise on Analytical Statics: With Numerous Examples*, vol. 1 of *Cambridge Library Collection - Mathematics*. Cambridge University Press, 2013.

[34] C. J. Boss, V. Srivastava, and H. K. Khalil, "Robust tracking of an unknown trajectory with a multi-rotor UAV: A high-gain observer approach," in *American Control Conference*, (Denver, CO), pp. 1429–1434, July 2020.

[35] H. K. Khalil, *High-Gain Observers in Nonlinear Feedback Control*. Society for Industrial and Applied Mathematics, 2017.